

# Slowly Divergent Drift in the Field-Driven Lorentz Gas

P. L. Krapivsky and S. Redner

Center for Polymer Studies and Department of Physics Boston University, Boston, MA 02215

The dynamics of a point charged particle which is driven by a uniform external electric field and moves in a medium of elastic scatterers is investigated. Using rudimentary approaches, we reproduce, in one dimension, the known results that the typical speed grows with time as  $t^{1/3}$  and that the leading behavior of the velocity distribution is  $e^{-|v|^3/t}$ . In spatial dimension  $d > 1$ , we develop an effective medium theory which provides a simple and comprehensive description for the motion of a test particle. This approach predicts that the typical speed grows as  $t^{1/3}$  for all  $d$ , while the speed distribution is given by the scaling form  $P(u, t) = \langle u \rangle^{-1} f(u/\langle u \rangle)$ , where  $u = |v|^{3/2}$ ,  $\langle u \rangle \sim \sqrt{t}$ , and  $f(z) \propto z^{(d-1)/3} e^{-z^2/2}$ . For a periodic Lorentz gas with an infinite horizon, *e. g.*, for a hypercubic lattice of scatterers, a logarithmic correction to the effective medium result is predicted; in particular, the typical speed grows as  $(t \ln t)^{1/3}$ .

PACS Numbers: 02.50.-r, 05.40.+j, 05.60+w

## I. INTRODUCTION

At the turn of the century, Drude developed a qualitative theory for electrical conduction in metals [1]. To establish a more solid basis for the Drude theory, Lorentz [2] suggested an idealized model for electron transport in metals in which: (i) electron-electron interactions are ignored, (ii) the background atoms are considered to be immobile spherical scatterers, and (iii) the electron-atom interaction is described by elastic scattering. This *Lorentz gas* [3] has played a large role in developing our understanding of diffusive transport in random media.

An important feature of the Lorentz gas is the independence of the electrons. This implies that the underlying Boltzmann equation for the evolution of the electron velocity distribution function (VDF) is linear. Because of this simplification, the Boltzmann equation has proven fruitful in understanding the properties of the Lorentz gas (see, *e. g.*, [4] and references therein). These investigations have established that, under relatively general conditions, a test particle moves diffusively and that its diffusivity can be computed in terms of the geometric properties of the background scatterers. The Lorentz model is also simple enough to be amenable to rigorous analytical studies (see, *e. g.*, [5–10]). In particular, for a periodic Lorentz gas in two dimensions with an “infinite” horizon (*i. e.*, there exist free trajectories of infinite length), anomalous diffusion of the form  $\langle r^2 \rangle \propto t \ln t$  has been proved [10]; this anomalous diffusion is also expected to hold in arbitrary dimension.

Paradoxically, much less is known about the problem which originally motivated the introduction of the Lorentz gas model, *i. e.*, the motion of a charged test particle in a scattering medium under the influence of a spatially uniform electric field. Lorentz himself constructed an approximate stationary solution to the Boltzmann equation by a perturbative expansion around the Maxwell-Boltzmann distribution [2]. From this solution, Lorentz reproduced the basic results of the Drude theory.

Unfortunately, the starting point of Lorentz’s analysis is erroneous. If the scattering is elastic (no dissipation), then an electron will necessarily gain kinetic energy as it accelerates in the field and a stationary asymptotic VDF will not exist. This dilemma motivated investigations of the field-driven Lorentz gas in which some form of dissipation is explicitly incorporated [11–13], so that it is possible to obtain Ohm’s law.

In the absence of dissipation, however, Piasecki and Wajnryb [14] were apparently the first to recognize the fundamental ramifications that arise from the non-stationarity of the system. From an exact solution to the Boltzmann equation in one dimension and an asymptotic solution for general  $d$  and with the crucial assumption of collision isotropy, they found: (i) the typical velocity,  $v_{\text{rms}}$ , grows with time as  $t^{1/3}$ , and (ii) the VDF has a non-stationary, but symmetric asymptotic form whose controlling factor is  $e^{-|v|^3/t}$ .

Our goal in the paper is to develop simple and physically transparent approaches to understand the behavior of the field-driven Lorentz gas. We begin by considering the one-dimensional system in Sec. II, where we substantially reproduce the results of Piasecki and Wajnryb [14]. We first construct a random walk argument to explain the mechanism that gives rise to the slow  $t^{1/3}$  increase of the root-mean-square velocity ( $v_{\text{rms}}$ ) with time. This argument relies on the assumption that each scattering event is spatially isotropic. This isotropy is a basic feature of elastic scattering from an immobile sphere only for the physical case of three dimensions [15]. If one postulate isotropic scattering even in one dimension, the results obtained can be expected to mimic three three-dimensional behavior. The Langevin and underlying Fokker-Planck equations for the speed distribution function (SDF) are also investigated to obtain both the time dependence of the typical speed and, more generally, the asymptotic form of the SDF. Finally, we develop a Lifshitz argument [16] to reproduce the asymptotic form of the SDF with minimal calculation.

In Sec. III, we study the field-driven Lorentz gas for arbitrary spatial dimension  $d$ . We argue that there are basic differences in the field-driven Lorentz gas for  $d = 1$  and for  $d > 1$ . In greater than one dimension, the freely-accelerated trajectory segments between scattering events are biased by the field, leading to anisotropy in the spatial position of the test particle at the next scattering event. To account for this bias in a relatively simple manner, we introduce an effective medium theory. In this description, a particle begins at the center of a “transparency” sphere of radius equal to the mean-free path. The particle freely accelerates until it reaches the sphere surface. This defines a collision, whereupon the test particle starts at the center of a new transparency sphere. We will generally assume isotropic scattering in each collision, a feature of elastic scattering from hard spheres in three dimensions. However, there is preferential backscattering for  $d < 3$  and preferential forward scattering for  $d > 3$ . This short-range correlation apparently does not affect the asymptotic motion of the test particle, so that we generally focus on isotropic scattering.

For isotropic scattering, it is simple to quantify the field-induced bias of the test particle as it moves within a transparency sphere. A random-walk argument of a similar spirit to that given in one dimension indicates that the influence of the bias is of the same order as the stochasticity caused by scattering. This implies that the SDF will obey one-parameter scaling. From the solution to the underlying Fokker-Planck equation, we find,  $P(u, t) \propto t^{-1/2} z^{(d-1)/3} \exp(-z^2/2)$ , where  $u = |v|^{3/2}$  is a convenient “speed” variable and the scaling variable  $z$  is proportional to  $u/t^{1/2}$ . We also extend the effective medium theory to the case where the mean-free path is chosen from a distribution  $\rho(\ell) \propto \ell^{-\mu}$ . This form accounts for the asymptotic distribution of mean free paths encountered by a test particle when (small) scattering centers are on regular lattice sites. As might be expected, when  $\mu > 3$ , corresponding to a finite second moment  $\langle \ell^2 \rangle$  of  $\rho(\ell)$ , the transport of the test particle is nearly identical to the case where the mean-free path is fixed. However for  $\mu < 3$ , *i. e.*, for a distribution  $\rho(\ell)$  with  $\langle \ell^2 \rangle = \infty$ , faster asymptotic transport arises. The borderline case of  $\mu = 3$  corresponds to a lattice array of scatterers such that an infinite horizon arises, and logarithmic corrections in the transport laws are predicted to occur.

In Sec. IV, we present Monte Carlo simulation results for the motion of a test particle in the two-dimensional effective medium. When the radius of the transparency circle is fixed, we obtain excellent agreement between simulation results and our theoretical predictions for the case of isotropic scattering. For simulations based on the correct scattering law for hard circles in two dimensions, virtually identical results are obtained, *i. e.*, short range antipersistence appears to be asymptotically irrelevant. We also consider the case of a power-law distribution of radii for the transparency circle,  $\rho(\ell) \propto \ell^{-\mu}$ . While the

physically interesting case of  $\mu = 3$  corresponds to the borderline of applicability of our naive effective medium approach, numerical results indicate transport properties which are close to those obtained for a fixed radius transparency circle.

In Sec. V, we present a brief discussion and summary.

## II. LORENTZ GAS IN ONE DIMENSION

### A. Random Walk Argument for the RMS Velocity

Consider a sizeless test particle (electron) which moves with constant acceleration  $a = eE/m$ , where  $e$  and  $m$  are the electron charge and mass, and  $E$  is the electric field. The electron moves in a medium of equally spaced point scatterers with separation  $\ell$ . To mimic the behavior of a three-dimensional system with isotropic scattering, we allow the particle to hop with equal probability to its nearest neighbor on the left or the right after each collision. Thus the electron trajectory consists of freely accelerating segments which are punctuated by isotropic scattering events. This is simply an isotropic random walk, but with position- and direction-dependent time increments between successive steps.

We use this physical picture to compute the behavior of the typical velocity as a function of time. Energy conservation gives

$$\frac{1}{2}mv_n^2 - eEx_n = \text{const.} \quad (1)$$

where  $v_n$  and  $x_n$  refer to the electron velocity and position immediately after the  $n^{\text{th}}$  scattering event. We rewrite this as

$$v_{n+1}^2 - v_n^2 = \frac{2eE}{m}(x_{n+1} - x_n) = \pm \frac{2eE\ell}{m}. \quad (2)$$

Because of the postulated isotropic scattering,  $v_{n+1}^2 - v_n^2$  is equally likely to be positive or negative. Thus we conclude that  $v_n^2$  undergoes a simple random walk as a function of  $n$ , with an elementary step size given by  $v_0^2 \equiv 2eE\ell/m$ . As a result,

$$\langle v_n^2 \rangle = \sqrt{n} v_0^2, \quad \text{or} \quad v_{\text{rms}} = n^{1/4} v_0. \quad (3)$$

To determine the dependence of  $v_{\text{rms}}$  on time, we write the time increment between successive collisions as

$$dt_n \equiv t_{n+1} - t_n \approx \ell/v_n. \quad (4)$$

The last approximation applies when the typical speed is large so that the acceleration between scatterings can be neglected, an assumption which can be verified *a posteriori*. The total elapsed time for  $n$  collisions is therefore

$$t = \sum_{k=1}^n dt_k \sim \frac{\ell}{v_0} \int_1^n \frac{dk}{k^{1/4}} \sim \frac{\ell}{v_0} n^{3/4}. \quad (5)$$

Solving for  $n$  as a function of time and substituting into Eq. (3), gives the fundamental result

$$v_{\text{rms}} \sim v_0 \left( \frac{v_0 t}{\ell} \right)^{1/3} \sim (a^2 \ell t)^{1/3}. \quad (6)$$

It is instructive to compare the time dependence of  $v_{\text{rms}}$  with that of the average velocity in the field direction. The latter can be computed from the recursion relation

$$v_{n+1} \approx \pm v_n + a dt_n \approx \pm v_n + \frac{a\ell}{v_n}, \quad (7)$$

By isotropy, the factor of  $\pm 1$  occurs equiprobably for each scattering. Since the typical speed grows indefinitely, we again ignore the acceleration during the free flight between adjacent sites, so that  $v_{\text{drift}} \equiv \langle v_n \rangle \approx \langle (a\ell/v_{\text{rms}}) \rangle$ . As a function of time, this may be rewritten as

$$v_{\text{drift}}(t) \sim \left( \frac{a\ell^2}{t} \right)^{1/3}. \quad (8)$$

Thus the average drift velocity *decreases* with time, even though the rms velocity grows with time. Therefore the VDF becomes systematically more isotropic in the long time limit [14].

Finally, making use of Eq. (8), one can estimate the average displacement  $\langle x(t) \rangle$  in the field direction to be,

$$\langle x(t) \rangle \sim v_{\text{drift}}(t) t \sim (a\ell^2 t^2)^{1/3}. \quad (9)$$

Alternatively, this same result follows directly from energy conservation, Eq. (1), and the time dependence of  $v_{\text{rms}}(t)$  from Eq. (6).

## B. The Speed Distribution

We now derive the speed distribution function using simple approaches which obviate the need to solve the Boltzmann equation, as given in [14]. First consider the Langevin equation to describe how the typical speed depends on  $n$ . Since  $v_n^2$  is randomly incremented or decremented by a fixed amount  $v_0^2$  in a single collision, we may write, in the large- $n$  limit,

$$\frac{dv_n^2}{dn} = v_0^2 \eta(n), \quad (10)$$

where the noise has zero mean,  $\langle \eta(n) \rangle = 0$ , and is temporally uncorrelated,  $\langle \eta(n)\eta(n') \rangle = \delta(n - n')$ . Since we are interested in the  $n \rightarrow \infty$  limit, the continuum result for the above correlation function is appropriate. In this limit, the amplitude distribution of the noise is also Gaussian. Consequently, the Langevin equation yields a Gaussian distribution for  $v_n^2$  with a dispersion equal to  $nv_0^4$  [17].

To determine the time dependence of the speed distribution, we transform from  $n$  to  $t$  by writing  $dt = \ell dn/|v_n|$ , so that

$$\frac{dv_n^2}{dn} = 2\ell \frac{d|v_n|}{dt}. \quad (11)$$

Next, we transform the dependence of the noise correlation from  $n$  to  $t$ . Writing  $\delta(n - n') = \delta(t - t') \frac{dt}{dn}$ , gives  $\langle \eta(n)\eta(n') \rangle = \langle \eta(t)\eta(t') \rangle \ell/|v|$ , so that  $\eta(n) = \eta(t) \sqrt{\ell/|v|}$ . Substituting this into the Langevin equation, Eq. (10), gives

$$\frac{d|v|}{dt} = \frac{v_0^2}{2\ell} \sqrt{\frac{\ell}{|v|}} \eta(t), \quad (12)$$

or

$$\frac{d|v|^{3/2}}{dt} = \frac{3v_0^2}{4\sqrt{\ell}} \eta(t). \quad (13)$$

Thus we conclude that the speed distribution function,  $P(u, t)$ , is Gaussian in  $u = |v|^{3/2}$ , with a dispersion which is proportional to  $v_0^4/\ell$ . Then the VDF is determined from the identity  $P(v, t)dv = P(u, t)du$  to yield

$$P(v, t) = \sqrt{\frac{|v|}{4\pi\ell a^2 t}} \exp \left[ -\frac{|v|^3}{9\ell a^2 t} \right] \quad (14)$$

An independent and appealing approach to obtain the VDF is by a Lifshitz tail argument [16]. This method is based on matching the assumed scaling form of the VDF with the “extreme” contribution that arises from a particle which is scattered in the field direction at each collision. This extreme tail can usually be estimated by elementary means, and matching this to the scaling form determines the VDF. Although this approach is heuristic, its advantages are simplicity and wide applicability.

Our starting point is to assume that the VDF can be written in the scaling form

$$P(v, t) \sim \frac{1}{v_{\text{rms}}} f(v/v_{\text{rms}}), \quad (15)$$

where the scaling function  $f(z)$  is expected to approach a constant as  $z \rightarrow 0$ , and vanish faster than any power law for  $z \rightarrow \infty$ . Generally, this large- $z$  asymptotic behavior has the quasi-exponential form

$$f(z) \sim \exp(-z^\delta), \quad (16)$$

which defines the “shape” exponent  $\delta$  of the distribution.

Let us now consider the trajectory in which the test particle is perpetually scattered parallel to the field, so that its speed is simply  $v = at$ . Substituting into Eq. (16) and using Eq. (6) for  $v_{\text{rms}}$  gives,

$$P(v = at, t) \sim e^{-(at/(a^2\ell t)^{1/3})^{\delta/3}} = e^{-(at^2/\ell)^{\delta/3}}. \quad (17)$$

On the other hand, the probability  $P_n$  that  $n$  scattering events are all parallel to the field equals  $2^{-n}$ . For this uniformly accelerated motion, the correspondence between  $n$  and the time is simply given by  $at^2/2 = n\ell$ . Thus writing  $P_n$  as a function of time and matching with the argument of the exponential in Eq. (17), gives  $\delta = 3$ , in agreement with the exact solution [14]. Parenthetically, if we define a size exponent  $\nu$  through  $v_{\text{rms}} \sim t^\nu$ , then the general scaling relation [18] between the size and shape exponents,  $\delta = (1-\nu)^{-1}$ , fails for the field-driven Lorentz gas.

### III. LORENTZ GAS IN GREATER THAN ONE DIMENSION

#### A. Effective Medium Approximation

The field-driven Lorentz gas in greater than one dimension presents a variety of theoretical and computational challenges. Numerical simulations of the dissipationless system are prone to large fluctuations and quantitative conclusions are not readily obtained [11]. Because of this computational difficulty and also because dissipation arises in any physical realization of the Lorentz gas, simulation work has primarily focused on the field-driven system with dissipation. This is achieved by either allowing for inelasticity in collision events [12], or by introducing a “thermostat” which continuously extracts energy from the particle during its free motion to maintain a constant kinetic energy [11,19]. While much is known about these dissipative systems [19,20], our interest is in the nonstationary behavior of dissipationless system. In particular, we wish to understand how the typical speed of a test particle grows with time and the form of the resulting SDF.

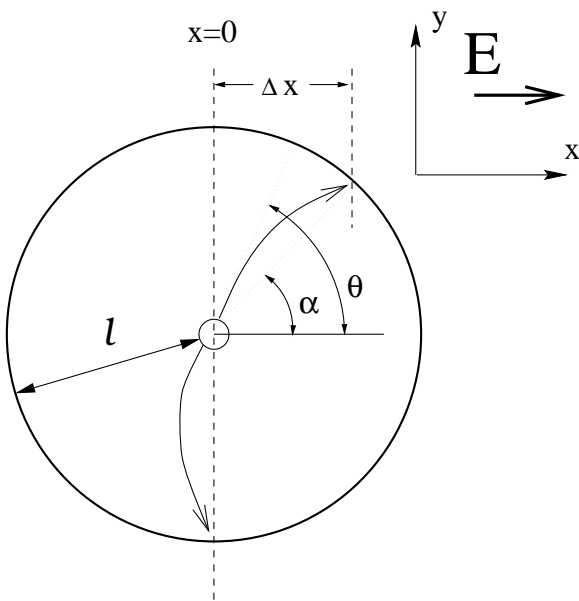


FIG. 1. “Transparency” sphere that surrounds a scatterer. After a scattering event, the test particle moves freely on a parabolic trajectory until the next collision at the sphere boundary. The initial and final angular position of the test particle,  $\theta$  and  $\alpha$ , respectively, are indicated. The critical trajectory is defined by the condition that the final longitudinal position of the test particle is at  $x = 0$ .

Because of the inherent difficulties in describing the motion of a test particle in a regular lattice of scatterers, we introduce an effective medium approximation in which the true trajectory is replaced by an effective, but physically equivalent, trajectory whose properties are readily calculable (Fig. 1). We assume that immediately after each scattering event, the test particle starts at the center of a transparency sphere of radius equal to the mean-free path  $\ell$ . The test particle then freely accelerates until the next collision when the surface of this sphere is reached. The collision point defines the center of the next transparency sphere. This construction is repeated to generate a particle trajectory which consists of parabolic segments (the biased free-particle motion between collisions), which are punctuated by collision events. We assume isotropic scattering so that the outgoing particle direction is randomized. This isotropy actually occurs for hard-sphere scattering only in three dimensions. An elementary computation shows that there is preferential back scattering for  $d < 3$  (with complete back scattering for  $d = 1$ ), and preferential forward scattering for  $d > 3$ . However, this persistence for  $d > 3$  or antipersistence for  $d < 3$  appears to be asymptotically negligible (see below).

#### B. The Typical Speed

To estimate the typical speed, we need to quantify the deflection of a trajectory during free flight. As we shall show, this leads to an effective bias which vanishes as the inverse square of the particle speed. Let us define trajectories whose collision points are in the hemisphere  $x > 0$  as positively biased and *vice versa*. Separating these trajectories is a “critical” trajectory, in which the next collision point is also at  $x = 0$  (Fig. 1). (This critical trajectory exists only if the initial speed satisfies  $v > v_0/\sqrt{2}$ ; otherwise all trajectories are deflected towards increasing  $x$ ) However, since the typical speed grows as a power law in time, the role of trajectories in which the speed at some stage is too small to define a critical trajectory is expected to be negligible.

By elementary mechanics, the inclination angle of this critical trajectory is given by

$$\theta = \frac{1}{2} \sin^{-1} \left( -\frac{a\ell}{v^2} \right) \approx \frac{\pi}{2} + \left( \frac{v_0}{2v} \right)^2, \quad \text{as } \frac{v_0}{v} \rightarrow 0. \quad (18)$$

The longitudinal motion of the test particle can thus be viewed as a biased one-dimensional random walk, with

the bias at each step proportional to  $\epsilon \equiv (v_0/2v)^2$ . Following the same steps as those given in Eqs. (1) – (6), the velocity increment between scatterings is given by  $v_{n+1}^2 - v_n^2 = \pm v_0^2$ , but with the  $\pm$  sign now occurring with respective probabilities  $\frac{1}{2}(1 \pm a\epsilon)$ , where  $a$  is a dimension-dependent number of order unity. Thus, in addition to the stochastic particle motion given in Eq. (3), a deterministic contribution also arises. This latter component gives, for the  $n$  dependence of the speed,

$$\langle v_n^2 \rangle \propto n\epsilon v_0^2, \quad \text{or} \quad v_{\text{rms}} \propto (n\epsilon)^{1/2} v_0. \quad (19)$$

To determine the time dependence, we relate  $n$  at  $t$  by using

$$t = \sum_{k=1}^n dt_k \propto \ell \int_1^n \frac{dk}{(k\epsilon)^{1/2}} \propto \frac{\ell}{v_0} \sqrt{\frac{n}{\epsilon}}. \quad (20)$$

Solving for  $n$  as a function of  $t$ , substituting into Eq. (19), and eliminating the factor  $\epsilon$ , we find that the speed is given by

$$v_{\text{rms}}(t) \sim v_0 \left( \frac{v_0 t}{\ell} \right)^{1/3}. \quad (21)$$

This is the same time dependence as one dimension, where there is no deterministic bias in the motion. Fortuitously, the manifestations of the isotropic scattering and the field bias are of the same order in our effective medium theory. This coincidence leads to a distribution of speeds which can be described by single parameter scaling.

### C. The Speed Distribution

To determine the speed distribution, we adapt our approach used in one dimension. First, we derive the Langevin equation for the dependence of the typical speed on  $n$ , from which the underlying Fokker-Planck equation may be written and then solved.

In a time  $\Delta\tau$  after collision  $n$  (and before collision  $n+1$ ), the particle will be at

$$\vec{r} = v \Delta\tau \hat{n} + \frac{a \Delta\tau^2}{2} \hat{e} \quad (22)$$

with respect to the center of the transparency sphere. Here  $\hat{n}$  and  $\hat{e}$  are the unit vectors in the direction of motion after the scattering event and the electric field, respectively, *i. e.*,  $\vec{v}_n = v\hat{n}$  and  $\vec{E} = E\hat{e}$ . The next collision event takes place on the surface of the sphere  $\vec{r}^2 = \ell^2$ . Consequently, the time increment  $\tau$  between collisions is implicitly given by

$$\ell^2 = (v\tau)^2 + av\tau^3(\hat{n} \cdot \hat{e}) + \frac{a^2\tau^4}{4}. \quad (23)$$

The velocity change between collisions is found from energy conservation

$$v_{n+1}^2 - v_n^2 = 2a(\vec{r} \cdot \hat{e}) = 2av\tau(\hat{n} \cdot \hat{e}) + (a\tau)^2. \quad (24)$$

Combining Eqs. (23) and (24), the time increment can be eliminated to give the analog of Eq. (2)

$$v_{n+1}^2 - v_n^2 \approx 2a\ell(\hat{n} \cdot \hat{e}) + \frac{a^2\ell^2}{v^2} [1 - (\hat{n} \cdot \hat{e})^2]. \quad (25)$$

In Eq. (25) and below we ignore terms of order  $\mathcal{O}(v_0^6/v^4)$ . The first term in Eq. (25) is purely stochastic, because  $\langle \hat{n} \cdot \hat{e} \rangle = 0$ . Since  $\langle (\hat{n} \cdot \hat{e})^2 \rangle = 1/d$ , we may write this stochastic term in the form  $v_0^2 \eta(n)/\sqrt{d}$ . The second term in Eq. (25) has both deterministic and stochastic components, with the latter being negligible in the long time limit. The magnitude of the deterministic component is  $(a\ell/v)^2(1 - 1/d) = (d-1)v_0^4/4v^2d$ . Thus we obtain the Langevin equation,

$$\frac{dv_n^2}{dn} = \frac{d-1}{4d} \frac{v_0^4}{v^2} + \frac{v_0^2}{\sqrt{d}} \eta(n). \quad (26)$$

In one dimension, the deterministic term disappears and Eq. (26) coincides with Eq. (10).

Following the same steps as those given after Eq. (10), we eliminate  $n$  in favor of the time to transform the above equation to

$$\frac{d|v|^{3/2}}{dt} = \frac{3(d-1)v_0^4}{16\ell d} \frac{1}{|v|^{3/2}} + \frac{3v_0^2}{4\sqrt{\ell d}} \eta(t). \quad (27)$$

In this equation, the order of magnitudes of the systematic and stochastic terms on the right-hand side are identical. Thus  $|v|^{3/2}$  evolves by a biased random-walk process, but one in which the bias and the dispersion are of the same scale. This can be seen more clearly by writing the underlying Fokker-Planck equation for  $P(u, t)$ , where  $u \equiv |v|^{3/2}$ . Following the standard prescription [17], this Fokker-Planck equation is

$$\frac{\partial P}{\partial t} = \frac{9v_0^4}{16\ell d} \left[ \frac{\partial^2 P}{\partial u^2} - \frac{d-1}{3d} \frac{\partial}{\partial u} \left( \frac{P}{u} \right) \right]. \quad (28)$$

We apply scaling to solve this equation. Let us make the scaling ansatz

$$P(u, t) = \frac{1}{\langle u \rangle} f(z) \quad \text{with} \quad z \equiv u/\langle u \rangle. \quad (29)$$

Substituting Eq. (29) into the Fokker-Planck equation (28), writing the time and velocity derivatives in terms of the scaling variable, the partial differential equation can be separated into two ordinary differential equations. For the time dependence of  $\langle u \rangle$ , we obtain

$$\frac{d}{dt} \langle u \rangle^2 = \frac{9v_0^4}{8\ell d}. \quad (30)$$

This then gives a characteristic speed which is proportional to  $(v_0^4 t / \ell)^{1/3}$  or  $(a^2 t \ell)^{1/3}$ . For the dependence on the scaling variable, the scaling function obeys the ordinary differential equation

$$-f(z) - z f'(z) = f''(z) + \frac{d-1}{3} \left[ \frac{f(z)}{z^2} - \frac{f'(z)}{z} \right], \quad (31)$$

where the prime denotes differentiation with respect to  $z$ . One integration gives

$$f'(z) = \left( \frac{d-1}{3z} - z \right) f(z) + A, \quad (32)$$

where  $A$  is a constant. Since  $f(z)$  and its first derivative vanish faster than any power of  $z$  for  $z \rightarrow \infty$ ,  $A = 0$ . The solution to the resulting equation is

$$f(z) = \frac{2^{(4-d)/6}}{\Gamma((d+2)/6)} z^{(d-1)/3} e^{-z^2/2}. \quad (33)$$

The numerical coefficient is determined by the normalization condition  $\int_0^\infty f(z) dz = 1$ ,  $\Gamma(y)$  denotes the gamma function [21]. Notice that the existence of the scaling form for the SDF hinged on the magnitude of the bias vanishing as  $u^{-1}$ .

#### D. Distributed Mean-free Paths

In both the random walk approach for  $d = 1$  and the effective medium theory for  $d > 1$ , a mean-free path which has the fixed value  $\ell$  for each scattering event was an inherent feature. However, in the Boltzmann equation approach of Piasecki and Wajnryb [14], a Poisson distribution of mean-free paths is implicitly assumed. Moreover, there will be a distribution of mean-free paths in any real scattering medium. We therefore consider the physical effects that such a distribution has on transport properties. We consider a power law distribution of mean-free paths,

$$\rho(\ell) \sim \lambda^{\mu-1} / \ell^\mu, \quad (34)$$

since this form, for  $\mu = 3$ , corresponds [22–24] to the Lorentz gas in a scattering medium with an “infinite” horizon (*e. g.*, a square lattice of small scatterers). Probability theory [25,26] suggests that if the distribution is relatively sharp, the previous random walk arguments apply, while for a broad distribution, different transport behavior arises.

Let us first consider the effect of distributed mean-free paths in one dimension. That is, a new mean-free path is independently chosen from the above distribution after each scattering event. We allow  $\mu$  to be arbitrary, since this general situation is tractable. If the second moment of  $\rho(\ell)$  is finite, *i. e.*,  $\mu > 3$ , then the distribution of a sum of a large number of independent random variables,

each distributed according to  $\rho(\ell)$ , approaches a Gaussian and the random walk argument of Sec. II applies. In contrast, for  $\mu \leq 3$ , a Lévy distribution, whose index depends on  $\mu$  [25,26], emerges. Making use of well-known results [25,26] for Lévy distributions, we determine the  $n$ -dependence of  $v_{\text{rms}}$  to be (the analog of Eq. (3)),

$$v_n^2 \sim v_0^2 \times \begin{cases} \sqrt{n \ln n}; & \mu = 3, \\ n^{1/(\mu-1)}; & \mu < 3, \end{cases} \quad (35)$$

with  $v_0^2 = \lambda a$ . Repeating the calculational steps in Sec. II, we find, for the time dependence of  $v_{\text{rms}}(t)$

$$v_{\text{rms}}(t) \sim v_0 \times \begin{cases} \left[ \frac{v_0 t}{\lambda} \ln \left( \frac{v_0 t}{\lambda} \right) \right]^{1/3}; & \mu = 3, \\ \left( \frac{v_0 t}{\lambda} \right)^{1/(2\mu-3)}; & 2 < \mu < 3. \end{cases} \quad (36)$$

The average displacement in the field direction is thus given by  $\langle x(t) \rangle = v_{\text{rms}}(t)^2 / 2a$ , while the drift velocity is  $v_{\text{drift}}(t) = \langle x(t) \rangle / t$ . For  $\mu \leq 2$ , the first moment of  $\rho(\ell)$  diverges, so that the typical mean-free path is infinite. Consequently, collisions become irrelevant asymptotically, so that the typical velocity should grow linearly in time and an asymmetric velocity distribution should arise.

## IV. NUMERICAL SIMULATIONS

To test our theoretical predictions, we perform Monte-Carlo simulations of particle motion in a two dimensional effective medium. An important element in this simulation is determining where an arbitrary parabolic trajectory, which starts at the origin, intersects the circumference of a concentric circle. This involves the unwieldy solution of a quartic equation. However, since the typical speed grows with time, individual trajectory segments should deviate only slightly from straight lines, especially in the long time limit. Thus we compute the trajectory and the time between collisions in a perturbation series appropriate for the large speed limit. If the speed happens to fall below a preset threshold such that a strongly curved trajectory segment should arise, we impose the constraint that for this segment the particle is deflected exactly parallel to the field. Since the typical speed increases with time, this “reflecting” boundary condition in velocity space is anticipated to have a negligible influence on the long-time motion of the test particle.

Our simulation algorithm therefore consists of the following basic steps to compute the velocity and time increments between collisions. These steps are repeated to generate a single particle trajectory:

- If the speed is above a predetermined threshold,  $v_{\text{th}}$ , then:
  1. Choose a random scattering angle in the range  $0 \leq \theta \leq \pi$  (see Fig. 1).

- Determine the angular position  $\alpha$  of the particle when it hits the surface of the circle. From elementary mechanics, the angle  $\alpha$  is perturbatively given in the large velocity limit by

$$\alpha = \theta - \epsilon \sin \theta + \epsilon^2 \sin 2\theta + \dots, \quad (37)$$

with  $\epsilon = (v_0/2v)^2$ .

- From the angle  $\alpha$ , determine the change in the longitudinal position of the particle,  $\Delta x$ , and thereby determine the change in the speed of the particle by  $v_f^2 = v_i^2 + v_0^2 \Delta x / \ell$ . Here  $v_i$  is the speed of the particle as it begins from the center of the transparency circle, and  $v_f$  is the particle speed just before the collision at the circumference of the circle.
- Determine the time increment,  $\tau$ , associated with this trajectory. In the large velocity limit,  $\tau$  is perturbatively given by

$$\tau = \frac{1}{v} \left\{ 1 - \epsilon \cos \theta + \frac{5\epsilon^2}{2} (\cos^2 \theta - 1) + \dots \right\}. \quad (38)$$

Here  $\tau$  and  $v$  have been expressed in units of  $\ell/v_0$  and  $v_0$  respectively.

- If the speed is less than  $v_{\text{th}}$ , then, the scattering angle is taken to be  $\theta = 0$ . Consequently,  $v_f^2 = v_i^2 + v_0^2$  and  $\tau = 2$ .

Clearly, the sharp difference in the update of the particle motion for initial speed smaller or larger than the threshold is a crude approximation. One can straightforwardly construct more accurate, but more cumbersome rules to integrate over low-speed trajectory segments. However, since these segments are relatively unlikely, this refinement was not pursued. Because of the arbitrariness in the integration of the low-speed segments, the actual value of  $v_{\text{th}}$  is also somewhat arbitrary and we chose  $v_{\text{th}} = v_0$ . This appears to provide a relatively good compromise between accuracy and limiting the range over which the arbitrary reflecting boundary condition is imposed. To appreciate the numerical implications, consider, for example,  $v = v_{\text{th}}$ . For this case, the maximum possible deviation between the initial and final angular position of the trajectory arises when  $\theta \approx 111.5^\circ$ , with  $\alpha - \theta \approx -15.8^\circ$ . For  $v = 2v_{\text{th}}$ , the maximum deviation point occurs when  $\theta \approx 97^\circ$ , with  $\alpha - \theta \approx -3.7^\circ$ . Thus the effect of the curvature in the individual trajectory segments should typically be small.

We also performed a more faithful simulation for two dimensions in which the correct hard-circle scattering is implemented. In place of step 1 given above, we assume that just before the  $n^{\text{th}}$  collision, with incidence angle  $\alpha_{n-1}$  (see Fig. 1), the test particle uniformly illuminates the cross-section of the scatterer which is taken

to be a circle of radius  $r$ . After specular reflection by the scatterer, the difference between the incident and final angles is  $d\psi = \pi - 2\sin^{-1}(b/r)$ , where the impact parameter  $b$  is uniformly distributed between  $\pm r$ . This angular deflection is used to compute the outgoing angle  $\theta_n = \alpha_{n-1} + d\psi$ , and the corresponding incoming angle  $\alpha_n$ . Our simulation results for this more faithful implementation of hard-circle scattering are virtually identical to those from isotropic scattering. Because of this agreement, and also for simplicity, our simulations concentrated on the case of isotropic scattering.

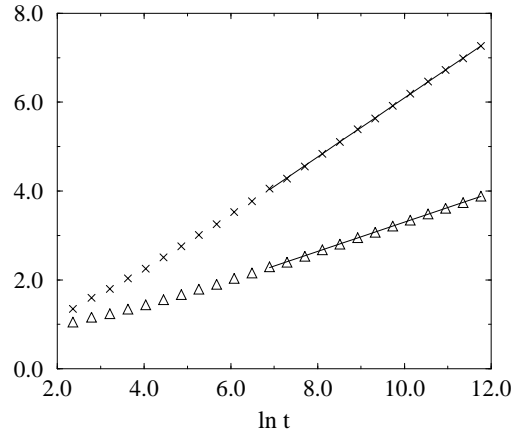


FIG. 2. Monte Carlo simulation results for 2000 walks of  $1.5^{29}$  steps in a two-dimensional effective medium. Shown are  $v_{\text{rms}}(t)$  ( $\Delta$ ), and the mean longitudinal position  $\langle x(t) \rangle$  ( $\times$ ). The straight lines represent the best fits to the data in the range  $1.5^{17} \leq t \leq 1.5^{29}$ .

Typical results from this Monte Carlo simulation with isotropic scattering are presented in Fig. 2. Shown are  $v_{\text{rms}}(t)$  and  $\langle x(t) \rangle$  on a double logarithmic scale based on 2000 trajectories of  $1.5^{29} \approx 127,834$  steps for the case where the transparency circle has a fixed radius. After some transient behavior, the data for  $t \gtrsim 500$  appear to be linear and a linear least-squares fits yields the respective slopes of 0.329 and 0.665, in excellent agreement with the respective theoretical predictions of 1/3 and 2/3. For true hard-circle scattering in two dimensions, our simulations gave the corresponding exponent estimates of 0.330 and 0.662. Thus the effect of the antipersistence in the particle motion truly appears to be irrelevant. In Fig. 3, we present corresponding results for the distribution of  $u = |v|^{3/2}$  at  $t = 1.5^{20}$  ( $\circ$ ),  $t = 1.5^{23}$  ( $\diamond$ ),  $t = 1.5^{26}$  ( $\nabla$ ), and  $t = 1.5^{29}$  ( $+$ ). The raw data has been scaled so that the abscissa is  $z = u/\langle u \rangle$ , while the ordinate is  $f(z) = \langle u \rangle P(u, t)$ . This scaled data at later times has then been smoothed by averaging over a small neighborhood to reduce fluctuations. These data compare well with the theoretical prediction  $f(z) = (2^{1/3}/\Gamma(2/3)) \times z^{1/3} e^{-z^2/2}$  (Fig. 3).

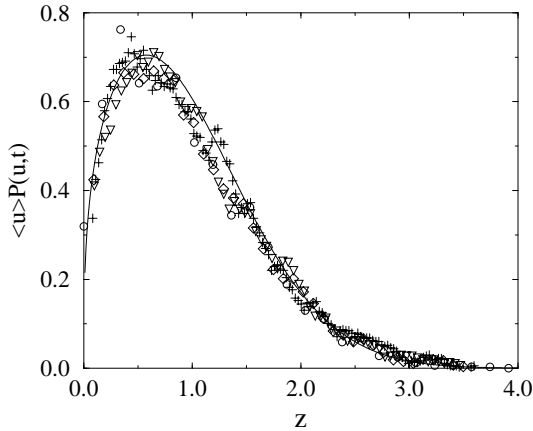


FIG. 3. Scaled distribution  $\langle u \rangle P(u, t)$  versus the variable  $z \equiv u / \langle u \rangle$ , where  $u = |v|^{3/2}$ . Representative data shown include  $t = 1.5^{20}$  ( $\circ$ ),  $t = 1.5^{23}$  ( $\diamond$ ), smoothed over a 3-site neighborhood,  $t = 1.5^{26}$  ( $\nabla$ ), smoothed over a 5-site neighborhood, and  $t = 1.5^{29}$  ( $+$ ), smoothed over a 7-site neighborhood. The curve is the theoretical prediction  $0.930 \dots \times z^{1/3} e^{-z^2/2}$ .

As discussed previously, a lattice array of scatterers leads to a power-law distribution of mean-free paths. We therefore also performed simulations of the effective medium where the radius of the next transparency circle is chosen from the distribution  $\rho(\ell) \sim \lambda^{\mu-1}/\ell^\mu$ , with  $\mu = 3$ . In this case, we found that the time dependence of  $v_{\text{rms}}(t)$  and  $\langle x(t) \rangle$  is quite close to that obtained for the case of a fixed-radius transparency circle. The data for  $t \gtrsim 1000$  appear to be linear on a double logarithmic scale, and a linear least-squares fits in this range yields the respective slopes of 0.340 and 0.671 (Fig. 4). For this case, however, the data for  $v_{\text{rms}}(t)$  and  $\langle x(t) \rangle$  exhibit a slight downward trend, a feature which could be attributed to a logarithmic correction. However, our data are insufficient to test for such a correction quantitatively.

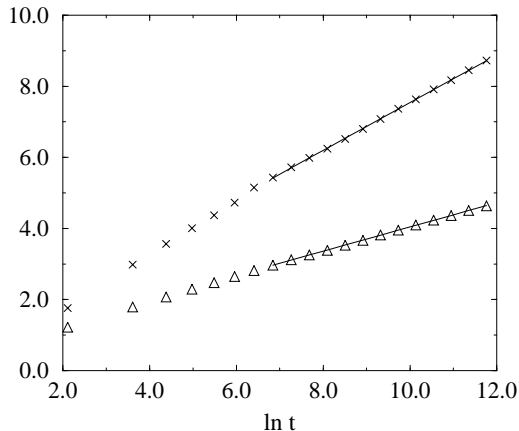


FIG. 4. Monte Carlo simulation results for 2000 walks of  $1.5^{29}$  steps in a two-dimensional effective medium in which the radius  $\ell$  of the transparency sphere is drawn from the distribution  $\rho(\ell) \propto \ell^{-3}$ . Shown are  $v_{\text{rms}}(t)$  ( $\Delta$ ), and the mean longitudinal position  $\langle x(t) \rangle$  ( $\times$ ). The straight lines represents the best fits to the data in the range  $1.5^{17} \leq t \leq 1.5^{29}$ .

The distribution of speeds also exhibits relatively good data collapse, but there are quantitative discrepancies between the shape of the scaling function and the prediction  $f(z) \approx 0.930 \dots \times z^{1/3} e^{-z^2/2}$  that fit the data for the case of a fixed-radius transparency sphere (Fig. 5)

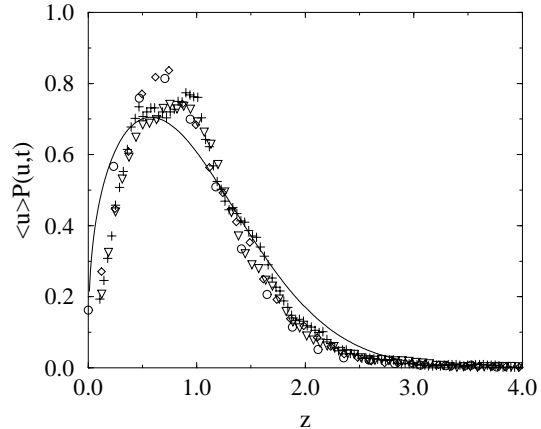


FIG. 5. Scaled distribution  $\langle u \rangle P(u, t)$  versus the variable  $z \equiv u / \langle u \rangle$ , where  $u = |v|^{3/2}$ . The radius  $\ell$  of the transparency sphere is drawn from the distribution  $\rho(\ell) \propto \ell^{-3}$ . Representative data shown include  $t = 1.5^{20}$  ( $\circ$ ),  $t = 1.5^{23}$  ( $\diamond$ ), smoothed over a 3-site neighborhood,  $t = 1.5^{26}$  ( $\nabla$ ), smoothed over a 5-site neighborhood, and  $t = 1.5^{29}$  ( $+$ ), smoothed over a 7-site neighborhood. The curve is  $0.930 \dots \times z^{1/3} e^{-z^2/2}$ .

## V. DISCUSSION AND SUMMARY

We have investigated the transport of a charged particle which is driven by a constant field in a dissipationless elastic and isotropic scattering medium – the field-driven Lorentz gas. A fundamental and intriguing feature of this system is that the transport is non-stationary. Namely, as a function of time, the typical velocity grows as  $t^{1/3}$ . Although this growth is unbounded, it is significantly slower than a linear time dependence that would occur in the absence of scattering. In one dimension, we have developed a random walk approach in which the particle hops to the right or left with equal probability at each scattering event. The time increment associated with each hop between neighboring scatterers is position and direction dependent, a feature which underlies the anomalous time dependence of the typical velocity and mean displacement.

Based on this random walk picture, we also obtained



the velocity distribution by first writing the Langevin equation for the evolution of the typical velocity and the underlying Fokker-Planck for the velocity distribution. We also constructed a Lifshitz tail argument which reproduced the correct behavior for the velocity distribution. The solution to the Fokker-Planck equation yields the Gaussian distribution in the variable  $u = |v|^{3/2}$ ,

$$P(u, t) \propto \frac{1}{\sqrt{t}} e^{-u^2/t}, \quad (39)$$

which, when written in terms of  $|v|$ , becomes

$$P(v, t) \propto \sqrt{\frac{|v|}{t}} e^{-|v|^3/t}. \quad (40)$$

Interestingly, this is similar, but not coincident with the asymptotic velocity distribution function

$$P(v, t) \propto \frac{1}{t^{1/3}} e^{-|v|^3/t}. \quad (41)$$

obtained by Piasecki and Wajnryb [14] from the Boltzmann equation approach. However, this approach implicitly assumes an “annealed” medium in which there is a Poisson distribution of distances between collision events. Thus, while our random walk and the Boltzmann approach are expected to give the same scaling of the typical speed with time, the form of the velocity distribution from the two approach should not be expected to coincide.

Our random walk argument can also be applied to the interesting case of an alternating electric field  $E(t) = E_0 \sin(\omega t)$  to give the counterintuitive result that the combination of an AC field and isotropic scattering leads to unbounded growth in the speed. This growth arises precisely because of the isotropy in the scattering events. When the time between collisions becomes less than the time for the field to reverse, then the direction of the field becomes irrelevant. Consequently, our random walk argument for a DC field directly applies and  $v_{\text{rms}}$  grows without bound in time. The validity of this statement depends only on the existence of a well-defined typical magnitude for the field. Thus for an AC external electric field, the scatterers assist in the absorption of field energy by the test particle. In contrast, in an AC field with no scattering, a test particle merely follows the field and the typical speed is bounded.

In higher dimensions, we introduced an effective medium approximation which provides a simple and physically appealing description for the motion of a charged test particle. This approximation posits that the test particle moves a fixed radial distance along a parabolic field-biased trajectory within a “transparency” sphere and that an isotropic collision event occurs when the particle reaches the surface of this sphere. The assumption of scattering when a particle moves a fixed radial distance implies an annealed medium. Thus one might expect a relatively close connection between the effective medium and the Boltzmann equation approaches.

However, because of the bias in the free-particle trajectory segments, an initially isotropic distribution of outgoing particle directions immediately after one scattering event becomes anisotropic at the next scattering. Within an equivalent one-dimensional random walk description of the test particle motion, this anisotropy can be described in terms of an effective bias which is proportional to  $1/v^2$ . The logical consequences of this feature again leads to a typical speed which again grows as  $t^{1/3}$ , just as in one dimension.

The effect of the field-induced bias is more pronounced in the behavior of the speed distribution, however. Following a similar approach as that given for one dimension, the solution to the Fokker-Planck equation for  $u = |v|^{3/2}$  is

$$P(u, t) \propto \frac{1}{\sqrt{t}} \left( \frac{u}{\sqrt{t}} \right)^{(d-1)/3} e^{-u^2/t}, \quad (42)$$

which, when written in terms of  $|v|$  gives

$$P(v, t) \propto \frac{|v|^{d/2}}{t^{(d+2)/6}} e^{-|v|^3/t}, \quad (43)$$

while the corresponding result of Piasecki and Wajnryb is

$$P(v, t) \propto \frac{|v|^{d-1}}{t^{d/3}} e^{-|v|^3/t}. \quad (44)$$

While these two forms agree for  $d = 2$ , the coincidence is unexpected. The Boltzmann approach explicitly builds in isotropy in the collision events and in the intervening particle motion, while the effective medium explicitly accounts for the field-induced bias between scattering events.

An attractive aspect of the effective medium approach is that it can be easily generalized to a distribution of mean-free paths, a feature which arises in a lattice realization of the Lorentz gas. Such a distribution may be accounted for by a power-law distribution of sphere radii  $\rho(\ell) \propto \ell^{-\mu}$ , with  $\mu = 3$ . This represents a marginal case between the regime where distributed radii appear to have no effect, for  $\mu > 3$ , to the case where the scaling of the mean speed with time is affected, for  $2 < \mu < 3$ . Our numerical simulations indicate that the case of  $\mu = 3$  leads to behavior similar to that of no dispersion in the sphere radii. However, the applicability of either the Boltzmann equation approach or our effective medium description to a lattice realization of the Lorentz gas has yet to be tested.

We thank R. S. Chivukula for a helpful discussion and J. Machta for particularly useful advice about hard-sphere scattering and related suggestions. This research was supported in part by the NSF (grants DMR-9219845 & DMR-9632059), and by the ARO (grant DAAH04-93-G-0021).

- 
- [1] P. Drude, *Annalen der Phys.* **1**, 566 (1900); *Annalen der Phys.* **3**, 369 (1900).
- [2] H. A. Lorentz, *Arch. Neerl.* **10**, 336 (1905); reprinted in *Collected Papers* (Martinus Nijhoff, The Hague, 1936), Vol. III, p. 180.
- [3] Sometimes, the Lorentz gas is called a Galton board, see e. g., M. Kac, *Scientific American* **211**, 92 (1964).
- [4] E. H. Hauge, in *Transport Phenomena*, edited by G. Kirzchenow and J. Marro (Lecture Notes in Physics, Springer-Verlag, Berlin, 1974), Vol. 31, p. 337.
- [5] L. A. Bunimovich and Ya. G. Sinai, *Comm. Math. Phys.* **78**, 247 (1980); L. A. Bunimovich and Ya. G. Sinai, *Comm. Math. Phys.* **78**, 479 (1981).
- [6] J. Machta and R. Zwanzig, *Phys. Rev. Lett.* **50**, 1959 (1983).
- [7] B. Friedman and R. F. Martin, *Phys. Lett. A* **105**, 23 (1984); *Physica D* **30**, 219 (1988).
- [8] J. Machta and B. Reinhold, *J. Stat. Phys.* **42**, 949 (1986).
- [9] L. A. Bunimovich, Ya. G. Sinai, N. I. Chernov, *Russ. Math. Surv.* **46**, 47 (1991).
- [10] P. Bleher, *J. Stat. Phys.* **66**, 315 (1992).
- [11] B. Moran, W. G. Hoover, and S. Bestiale, *J. Stat. Phys.* **48**, 709 (1987).
- [12] A. Lue and H. Brenner, *Phys. Rev. E* **47**, 3128 (1993).
- [13] N. I. Chernov, G. L. Eying, J. L. Lebowitz, and Ya. G. Sinai, *Phys. Rev. Lett.* **70**, 2209 (1993).
- [14] J. Piasecki and E. Wajnryb, *J. Stat. Phys.* **21**, 549 (1979).
- [15] L. D. Landau and E. M. Lifshitz, *Mechanics*, (Pergamon Press, Oxford, 1976).
- [16] I. M. Lifshitz, S. A. Gredeskul, and L. A. Pastur, *Introduction to the Theory of Disordered Systems* (Wiley, New York, 1988).
- [17] N. G. Van Kampen, *Stochastic Processes in Physics and Chemistry*, (North-Holland, Amsterdam, 1984).
- [18] M. E. Fisher, *J. Chem. Phys.* **44**, 616 (1966).
- [19] D. J. Evans and G. P. Morriss, *Statistical Mechanics of Nonequilibrium Liquids* (Academic, London, 1990).
- [20] N. I. Chernov, G. L. Eyink, J. L. Lebowitz, and Ya. G. Sinai, *Commun. Math. Phys.* **154**, 569 (1993).
- [21] M. Abramowitz and I. A. Stegun, *Handbook of Mathematical Functions* (Dover, New York, 1965).
- [22] L. A. Bunimovich, *Zh. Exsp. Theor. Fiz.* **89**, 1452 (1985) [*Sov. Phys. JETP* **62**, 842 (1985)].
- [23] J.-P. Bouchaud and P. Le Doussal, *J. Stat. Phys.* **41**, 225 (1985).
- [24] A. Zacherl, T. Geisel, J. Nierwetberg, and G. Radons, *Phys. Lett. A* **114**, 317 (1986).
- [25] B. V. Gnedenko and A. N. Kolmogorov, *Limit Distributions for Sums of Independent Random Variables* (Addison Wesley, Reading, MA, 1954).
- [26] J.-P. Bouchaud and A. Georges, *Phys. Reports* **195**, 127 (1990).